Journal of Molecular Structure 1008 (2012) 102–107

Contents lists available at SciVerse ScienceDirect

Journal of Molecular Structure

journal homepage: www.elsevier.com/locate/molstruc

Structural studies on acetophenone- and benzophenone-derived thiosemicarbazones and their zinc(II) complexes

Karina S.O. Ferraz [a], Nayane F. Silva [a], Jeferson G. Da Silva [a], Nivaldo L. Speziali [b], Isolda C. Mendes [c], Heloisa Beraldo [a,*]

[a] Departamento de Química, Universidade Federal de Minas Gerais, 31270-901 Belo Horizonte, MG, Brazil
[b] Departamento de Física, Universidade Federal de Minas Gerais, 31270-901 Belo Horizonte, MG, Brazil
[c] Escola de Belas Artes, Departamento de Artes Plásticas, Universidade Federal de Minas Gerais, 31270-901 Belo Horizonte, MG, Brazil

ARTICLE INFO

Article history:
Received 19 September 2011
Received in revised form 21 November 2011
Accepted 21 November 2011
Available online 28 November 2011

Keywords:
Thiosemicarbazones
Zinc(II) complexes
Crystal structures

ABSTRACT

In the present work *N*(3)-*meta*-chlorophenyl- (HAc3*m*Cl, **1**) and *N*(3)-*meta*-fluorphenyl- (HAc3*m*F, **2**) acetophenone thiosemicarbazone, and *N*(3)-*meta*-chlorophenyl- (HBz3*m*Cl, **3**) and *N*(3)-*meta*-fluorphenyl- (HBz3*m*F, **4**) benzophenone thiosemicarbazone were obtained, as well as their zinc(II) complexes $[Zn(Ac3mCl)_2]$ (**5**), $[Zn(Ac3mF)_2]$ (**6**), $[Zn(Bz3mCl)_2]$ (**7**) and $[Zn(Bz3mF)_2]$ (**8**). Upon re-crystallization in DMSO:acetone conversion of **8** into $[Zn(Bz3mF)_2]\cdot(DMSO)$ (**8a**) occurred. The crystal structures of **2**, **5** and **8a** were determined.

1. Introduction

Thiosemicarbazones are an important class of compounds with innumerous biological applications as antitumor, antiviral and antimicrobial agents [1]. α(*N*)-heterocyclic thiosemicarbazones were extensively investigated for their antitumor and cytotoxic activities, which were related to their ability to inhibit ribonucleoside diphosphate reductase (RDR), a key enzyme involved in DNA synthesis [2].

Thiosemicarbazones act as ligands in coordination chemistry in different ways [3]. They can bind metal ions as bidentate NS- or tridentate NNS-donor ligands forming five-membered chelate rings. Transition metal complexes of thiosemicarbazones are of considerable interest in chemistry because of their bioinorganic relevance [4,5].

Zinc is the second most prominent trace metal in the human body after iron. Zinc(II) ions are essential for all forms of life. In humans, they have catalytic and structural functions in an estimated 3000 zinc proteins [6]. Zinc is cytoprotective and suppresses apoptotic pathways. Zinc plays a role in brain, where it has a specific function as a neuromodulator in addition to its other typical cellular functions [7].

Considering the wide pharmacological versatility of thiosemicarbazones and the important role of zinc(II) in biological processes, it is of interest to prepare new zinc(II) complexes with thiosemicarbazones. In fact zinc(II) complexes with this class of ligands proved to exhibit cytotoxic, antiproliferative [3,8] and antimicrobial activities [9], among others.

In the present work *N*(3)-*meta*-chlorophenyl acetophenone-(HAc3*m*Cl) and *N*(3)-*meta*-fluorphenyl acetophenone-(HAc3*m*F) thiosemicarbazones and *N*(3)-*meta*-chlorophenyl benzophenone-(HBz3*m*Cl) and *N*(3)-*meta*-fluorphenyl benzophenone-(HBz3*m*F) thiosemicarbazones (see Fig. 1) were obtained as well as their zinc(II) complexes. The spectral and structural properties of the studied compounds were investigated.

2. Experimental section

2.1. Materials and measurements

Chemicals: acetophenone (Aldrich), benzophenone (Fluka), hydrazine hydrate (Aldrich), sulfuric acid (Synth), triethylamine (Merck), zinc(II) chloride (Vetec). Solvents: absolute ethanol (Synth), methanol (Synth), acetone (Synth), dimethylsulfoxide (Synth), DMSO-d_6 (CIL) and diethylether (Synth).

Partial elemental analyses were performed on a Perkin Elmer CHN 2400 analyzer. Infrared spectra were recorded on a Perkin–Elmer FT-IR Spectrum GX spectrometer using CsI pellets; an YSI model 31 conductivity bridge was employed for molar conductivity measurements. NMR spectra were obtained at room temperature with a Brucker DRX-200 Avance (200 MHz) spectrometer using deuterated dimethyl sulfoxide (DMSO-d_6) as the solvent and tetramethylsilane (TMS) as internal reference.

* Corresponding author. Tel.: +55 31 34095740; fax: +55 31 34095700.
E-mail address: hberaldo@ufmg.br (H. Beraldo).

0022-2860/$ - see front matter © 2011 Elsevier B.V. All rights reserved.
doi:10.1016/j.molstruc.2011.11.035

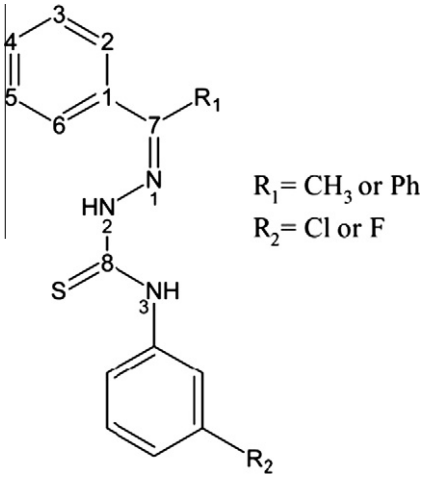

Fig. 1. General structure of *N*(3)-phenyl-acethophenone- and benzophenone-derived thiosemicarbazones.

The X-ray diffraction measurements were carried out on a GEMINI-Ultra diffractometer. The data collection, cell refinement results, and data reduction were performed using the CRYSALISPRO software [10]. Semi-empirical from equivalents absorption correction method was applied [10]. The structures were solved by direct methods using SHELXS-97 [11]. Full-matrix least-squares refinement procedure on F^2 with anisotropic thermal parameters was carried on using SHELXL-97 [11]. Positional and anisotropic atomic displacement parameters were refined for all non-hydrogen atoms. Hydrogen atoms were placed geometrically and the positional parameters were refined using a riding model.

2.2. Syntheses

2.2.1. Synthesis of N(3)-meta-chlorophenyl- (HAc3mCl, **1**) and N(3)-meta-fluorphenyl- (HAc3mF, **2**) acetophenone thiosemicarbazone, and N(3)-meta-chlorophenyl- (HBz3mCl, **3**) and N(3)-meta-fluorphenyl- (HBz3mF, **4**) benzophenone thiosemicarbazone

The thiosemicarbazones were prepared by a method described in the literature [12]. A solution of hydrazine hydrate (10 mmol) in methanol (10 mL) was added to a solution of the desired isothiocianate (10 mmol in 10 mL of methanol). The reaction mixture was kept under stirring in an ice bath for 15 min. Thereafter, the reaction was stirred for 24 h at room temperature. The obtained thiosemicarbazide was filtered and washed with diethyl ether. The thiosemicarbazide (5 mmol) was then dissolved in methanol (10 mL) and mixed to a solution of acetophenone or benzophenone (5 mmol) in methanol (10 mL) with addition of two drops of concentrated sulfuric acid. The reaction mixture was kept under stirring for 24 h at room temperature. The resulting solids were filtered off, washed with methanol and ether and dried in vacuum.

*2.2.1.1. N(3)-meta-chlorophenyl-acetophenone-thiosemicarbazone, HAc3mCl (**1**).* White solid. Yield: 68%. IR (KBr, cm^{-1}): ν(N3—H) 3295 s, ν(N2—H) 3239 m, ν(C=N) 1520 s, ν(C=S) 793 w. UV–Vis (DMF, cm^{-1}): 32362. The main signals in ^{1}H NMR (DMSO-d_6): δ (ppm) = 8.04–7.99 (1H, d, H(2), H(6)); 7.44–7.39 (1H, t, H(3), H(4), H(5)); 7.79 (1H, s, H(10)); 7.28–7.24 (1H, d, H(12); 7.43–7.39 (1H, t, H(13)); 7.61–7.57 (1H, d, H(14)); 10.77 (1H, s, N(2)H); 10.12 (1H, s, N(3)H). ^{13}C NMR (DMSO-d_6): δ (ppm) = 176.83, C8=S; 132.08, C7=N; 149.51, C1; 126.85, (C2, C6); 128.19, (C3, C5 and C4); 140.58, C9; 125.11, C10; 124.92, C12; 14.49, C15. $^nJ(^1H)$: 6.01, ^1J(H2, H3); 3.26, ^1J(H6, H5); 3.26, ^2J(H2, H4); 8.07, ^1J(H12, H13); 8.07, ^1J(H13, H14).

*2.2.1.2. N(3)-meta-fluorphenyl-acetophenone-thiosemicarbazone, HAc3mF (**2**).* White solid. Yield: 99%. IR (KBr, cm^{-1}): ν(N3—H) 3299 s, ν(N2—H) 3264 s, ν(C=N) 1520 s, ν(C=S) 787 w. UV–Vis (DMF, cm^{-1}): 32,573. The main signals in ^{1}H NMR (DMSO-d_6): δ (ppm) = 8.03–7.98 (1H, d, H(2), H(6)); 7.44–7.33 (1H, t, H(3), H(5) and H(4)); 7.67–7.61 (1H, s, H(10)); 7.04 (1H, d, H(12); 7.44–7.33 (1H, t, H(13)); 7.48–7.33 (1H, d, H(14)); 2.39 (3H, s, H(15)); 10.50 (1H, s, N(2)H); 9.01 (1H, s, N(3)H). ^{13}C NMR (DMSO-d_6): δ (ppm) = 176.71, C8=S; 137.31, C7=N; 149.49, C1; 126.83, (C2, C6); 128.19, (C3, C5); 129.32, C4; 140.90–140.68, C9; 112.35–111.86, C10; 111.86–111.46, C12; 14.48, C15. $^nJ(^1H)$: 6.17, ^1J(H2, H3); 2.73, ^2J(H2, H4); 11.15, ^1J(H12, H13); 2.23 ^2J(H12, H14).

*2.2.1.3. N(3)-meta-chlorophenyl-benzophenone-thiosemicarbazone, HBz3mCl (**3**).* White solid. Yield: 70%. IR (KBr, cm^{-1}): ν(N3—H) 3342 s, ν(N2—H) 3292 s, ν(C=N) 1588 s, ν(C=S) 804 w. UV–Vis (DMF, cm^{-1}): 31,348. The main signals in ^{1}H NMR (DMSO-d_6): δ (ppm) = 7.74–7.65 (1H, d, H(2), H(6)); 7.45–7.37 (1H, t, H(3), H(5) and H(4)); 7.74–7.65 (1H, s, H(10)); 7.31–7.27 (1H, d, H(12); 7.45–7.37 (1H, t, H(13)); 7.60–7.56 (1H, d, H(14)); 10.50 (1H, s, N(2)H); 9.01 (1H, s, N(3)H). ^{13}C NMR (DMSO-d_6): δ (ppm) = 176.01, C8=S; 136.14, C7=N; 150.39, C1; 128.37, (C2, C6); 129.73, (C3, C5); 129.99, C4; 140.31, C9; 127.89, C10; 125.34, C12. $^nJ(^1H)$: 7.29, ^1J(H12, H13); 7.92, ^1J(H13, H14).

*2.2.1.4. N(3)-meta-fluorphenyl-benzophenone-thiosemicarbazone, HBz3mF (**4**).* White solid. Yield: 88%. IR (KBr, cm^{-1}): ν(N3—H) 3302 s, ν(N2—H) 3198 s, ν(C=N) 1546 s, ν(C=S) 780 w. UV–Vis (DMF, cm^{-1}): 31,446. The main signals in ^{1}H NMR (DMSO-d_6): δ (ppm) = 7.75–7.71 (1H, d, H(2), H(6)); 7.43–7.39 (1H, t, H(3), H(5) and H(4)); 7.58 (1H, s, H(10)); 7.07 (1H, d, H(12); 7.68–7.65 (1H, t, H(13)); 7.68–7.65 (1H, d, H(14)); 10.52 (1H, s, N(2)H); 9.03 (1H, s, N(3)H). ^{13}C NMR (DMSO-d_6): δ (ppm) = 175.93, C8=S; 150.32, C7=N;, C1; 127.62, (C2, C6); 128.37, (C3, C5); 129.97, C4; 140.65–140.43, C9; 112.69–112.34, C10; 112.20–111.93, C12. $^nJ(^1H)$: 6.08, ^1J(H12, H13); 2.53, ^1J(H13, H14).

2.2.2. Synthesis of the zinc(II) complexes with N(3)-meta-chlorophenyl and N(3)-meta-fluorphenyl acetophenone- and benzophenone-thiosemicarbazones

The zinc(II) complexes were obtained by refluxing an ethanol solution of the desired thiosemicarbazone with zinc(II) chloride and triethylamine in 1:1:1 ligand-to-metal-to-triethylamine molar ratio. The obtained solids were washed with ethanol and diethyl ether and then dried under vacuum.

*2.2.2.1. Bis[(N(3)-meta-chlorophenylacetophenone-thiosemicarbazonato)zinc(II)], [Zn(Ac3mCl)$_2$] (**5**).* Yellow solid. Yield: 74%. Anal. Calc. (MW 671.0) C, 53.70%; H, 3.91%; N, 12.52%. Found: C, 53.87%; H, 3.80%; N, 12.72.57%. Molar conductivity (1×10^{-3} mol L^{-1} DMF): 0.44 Ω^{-1} cm^2 mol^{-1}. IR (KBr, cm^{-1}): ν(N3—H) 3414 m, ν(C=N) 1490 s, ν(C=S) 762 w, ν(Zn—N) 423 m, ν(Zn—S) 367 m. UV–Vis (DMF, cm^{-1}): 33,783, 30,769. The main signals in ^{1}H NMR (DMSO-d_6): δ (ppm) = 7.57–7.53 (1H, d, H(2), H(6)); 7.34–7.14 (1H, t, H(3), H(5) and H(4)); 7.87 (1H, s, H(10)); 6.99–6.95 (1H, d, H(12); 7.34–7.14 (1H, t, H(13)); 7.53–7.44 (1H, d, H(14)); 9.42 (1H, s, N(3)H). ^{13}C NMR (DMSO-d_6): δ (ppm) = 167.05, C8=S; 132.61, C7=N; 137.30, C1; 127.34, (C2, C6); 128.16, (C3, C5); 142.33, C9; 120.81, C10; 119.36, C12; 21.18, C15. $^nJ(^1H)$: 7.25, ^1J(H2, H3); 7.57, ^1J(H12, H13); 8.31, ^1J(H13, H14).

*2.2.2.2. bis[(N(3)-meta-fluorphenylacetophenone-thiosemicarbazonato)zinc(II)], [Zn(Ac3mF)$_2$] (**6**).* Yellow solid. Yield: 73%. Anal. Calc. (MW 638.09) C, 56.47%; H, 4.11%; N, 13.17%. Found: C, 56.44%; H, 4.00%; N, 13.27%. Molar conductivity (1×10^{-3} mol L^{-1} DMF): 0.18 Ω^{-1} cm^2 mol^{-1}. IR (KBr, cm^{-1}): ν(N3—H) 3330 m, ν(C=N)

1500 s, ν(C=S) 756 w, ν(Zn—N) 418 m, ν(Zn—S) 349 m. UV–Vis (DMF, cm^{-1}): 31,152, 29,940. The main signals in ^1H NMR (DMSO-d_6): δ (ppm) = 7.65–7.53 (1H, d, H(2), H(6)); 7.33–7.19 (1H, t, H(3), H(5) and H(4)); 7.65 (1H, s, H(10)); 6.74 (1H, d, H(12); 7.33–7.19 (1H, t, H(13)); 7.33–7.19 (1H, d, H(14)); 9.43 (1H, s, N(3)H). ^{13}C NMR (DMSO-d_6): δ (ppm) = 167.11, C8=S; 137.30, C7=N; 159.64, C1; 127.34, (C2, C6); 128.19, (C3, C5); 142.82–142.59, C9; 106.75–106.22, C10; 107.85–107.76, C12. $^nJ(^1H)$: 8.04, ^1J(H12, H13).

*2.2.2.3. Bis[(N(3)-meta-chlorophenylbenzophenone-thiosemicarbazonato)zinc(II)], [Zn(Bz3mCl)$_2$] (**7**).* Yellow solid. Yield: 70%. Anal. Calc. (MW 795.13) C, 60.42%; H, 3.81%; N, 10.54%. Found: C, 60.14%; H, 3.80%; N, 10.57%. Molar conductivity (1×10^{-3} mol L^{-1} DMF): 0.09 Ω^{-1} cm^2 mol^{-1}. IR (KBr, cm^{-1}): ν(N3—H) 3320 m, ν(C=N) 1481 s, ν(C=S) 777 w, ν(Zn—N) 420 m, ν(Zn—S) 349 m. UV–Vis (DMF, cm^{-1}): 31,250, 27,778. The main signals in ^1H NMR (DMSO-d_6): δ (ppm) = 6.81 (1H, d, H(2), H(6)); 6.99–6.92 (1H, t, H(3), H(5)); 6.82 (1H, d, H(12); 7.50–7.45 (1H, t, H(13)); 7.24 (1H, d, H(14)); 9.42 (1H, s, N(3)H). ^{13}C NMR (DMSO-d_6): δ (ppm) = 168.06, C8=S; 132.63, C7=N; 136.67, C1; 129.27, (C2, C6); 129.49 (C3, C5); 141.94, C9; 120.94, C10; 117.64, C12. $^nJ(^1H)$: 8.03, ^1J(H12, H13); 8.42, ^1J(H13, H14).

*2.2.2.4. Bis[(N(3)-meta-fluorphenylbenzophenone-thiosemicarbazonato)zinc(II)], [Zn(Bz3mF)$_2$] (**8**).* Yellow solid. Yield: 74%. Anal. Calc. (MW 762.23) C, 63.03%; H, 3.97%; N, 11.03%. Found: C, 62.83%; H, 3.76%; N, 11.28%. Molar conductivity (1×10^{-3} mol L^{-1} DMF): 0.35 Ω^{-1} cm^2 mol^{-1}. IR (KBr, cm^{-1}): ν(N3—H) 3318 m, ν(C=N) 1481 s, ν(C=S) 755 w, ν(Zn—N) 419 m, ν(Zn—S) 349 m. UV–Vis (DMF, cm^{-1}): 29,851, 27,322. The main signals in ^1H NMR (DMSO-d_6): δ (ppm) = 7.50–7.47 (1H, d, H(2), H(6)); 7.40–7.36 (1H, t, H(3), H(5)); 6.58 (1H, d, H(12); 7.07 (1H, t, H(13)); 6.99–6.96 (1H, d, H(14)); 9.44 (1H, s, N(3)H). ^{13}C NMR (DMSO-d_6): δ (ppm) = 167.90, C8=S; 136.90, C7=N; 159.50, C1; 128.31, (C2, C6); 129.45 (C3, C5); 142.36–142.13, C9; 105.94–105.91, C10; 107.77–107.34, C12. $^nJ(^1H)$: 6.69, ^1J(H2, H3); 7.96, ^1J(H12, H13); 12.49, ^1J(H13, H14).

2.3. X-ray crystallography

Upon slow evaporation of **2**, **5** and **8** in 9:1 acetone/DMSO crystals of HAc3*m*F (**2**), [Zn(Ac3*m*Cl)$_2$] (**5**), and [Zn(Bz3*m*F)$_2$]·DMSO (**8a**) were formed and their crystal structures were determined using single-crystal X-ray diffractometry.

A summary of the crystals data, data collection details and refinement results are listed in Table 1. Molecular graphics and packing figures were prepared using ORTEP [13] and PLATON [14], respectively.

3. Results and discussion

3.1. Formation of the thiosemicarbazones and zinc(II) complexes

Formation of the thiosemicarbazones was confirmed by their IR, electronic and NMR spectra. Microanalyses and molar conductivity data indicated the formation of [Zn(Ac3*m*Cl)$_2$] (**5**), [Zn(Ac3*m*F)$_2$] (**6**), [Zn(Bz3*m*Cl)$_2$] (**7**), and [Zn(Bz3*m*F)$_2$] (**8**) in which two anionic thiosemicarbazones are attached to the zinc(II) center.

3.2. Characterization

3.2.1. IR spectra

In the infrared spectra of the thiosemicarbazones absorptions at 3342–3295 cm^{-1} were assigned to the ν(N—H) stretching vibrations [15]. The absence of the absorption attributed to ν(N2—H) in the spectra of the complexes is according to coordination of an anionic thiosemicarbazone [16,4].The band assigned to ν(C=N) at 1588–1520 cm^{-1} in the spectra of the thiosemicarbazones shifts to 1500–1481 cm^{-1} in the spectra of complexes (**5–8**) suggesting coordination of the imine nitrogen [17]. The absorption attributed to ν(C=S) at 804–780 cm^{-1} in the spectra of the free

Table 1
Crystal data and refinement results for HAc3*m*F (**2**), [Zn(Ac3*m*Cl)$_2$] (**5**) and [Zn(Bz3*m*F)$_2$]·DMSO (**8a**).

Identification code	(**2**)	(**5**)	(**8a**)
Empirical formula	$C_{16}H_{16}FN_3S$	$C_{30}H_{26}Cl_2N_6S_2Zn$	$C_{42}H_{36}F_2N_6OS_3Zn$
Formula weight (g mol^{-1})	301.38	670.96	840.32
Crystal system	Triclinic	Monoclinic	Triclinic
Space group	$P-1$	$C\,2/c$	$P-1$
Temperature (K)	293(2)	293(2)	250(2)
Radiation, λ (Å)	Mo Kα, 0.71073	Cu Kα, 1.54184	Mo Kα, 0.71073
θ Range for data collection	3.00–26.37	4.71–58.93	4.08–26.37
Limiting indices	$-6 \leqslant h \leqslant 7$, $-10 \leqslant k \leqslant 13$, $-14 \leqslant l \leqslant 13$	$-21 \leqslant h \leqslant 21$, $-9 \leqslant k \leqslant 10$, $-19 \leqslant l \leqslant 14$	$-13 \leqslant h \leqslant 13$, $-14 \leqslant k \leqslant 14$, $-22 \leqslant l \leqslant 22$
a (Å)	5.8624(2)	19.3896(16)	10.4751(2)
b (Å)	10.5083(4)	9.0743(5)	11.4047(2)
c (Å)	12.0065(4)	17.4434(14)	18.3352(4)
α (°)	74.714(3)	90	79.654(2)
β (°)	86.591(3)	104.534	75.821(2)
γ (°)	89.559(3)	90	71.934(2)
Volume (Å^3)	712.19(4)	2970.9(4)	2006.19(7)
F(000)	316	1376	868
Z/*D* calc. (mg m^{-3})	2/1.405	4/1.500	2/1.391
Absorption coefficient μ (mm^{-1})	0.235	4.371	0.819
Reflections collected	5414	9168	32790
Reflections unique/*R*(int)	2901/0.0218	2132/0.0467	8170/0.0305
Completeness to θ	99.9% (θ = 26.37)	100.0% (θ = 58.93)	99.6% (θ = 26.37)
Data/restraints/parameters	2901/0/181	2132/0/187	8170/168/588
Final *R* indices [$I > 2\sigma(I)$]	R_1 = 0.0430, wR_2 = 0.1071	R_1 = 0.0416, wR_2 = 0.1024	R_1 = 0.0324, wR_2 = 0.0839
R indices (all data)	R_1 = 0.0694, wR_2 = 0.1147	R_1 = 0.0646, wR_2 = 0.1180	R_1 = 0.0458, wR_2 = 0.0871
Goodness-of-fit on F^2	0.953	1.051	1.039
Largest difference in peak and hole (e Å^3)	0.368 and −0.263	0.252 and −0.273	0.733 and −0.433

thiosemicarbazones shifts to 777–755 cm^{-1} in the spectra of the complexes, indicating coordination through a thiolate sulfur [9,18,19]. New absorptions at 423–418 cm^{-1} and 367–349 cm^{-1} in the spectra of the complexes were assigned to ν(Zn—N) and ν(Zn—S), respectively [4,20,21]. Hence the infrared spectra indicate coordination through the N—S chelating system.

3.2.2. Electronic spectra

The electronic spectra of the acetophenone-derived thiosemicarbazones show an absorption at ca. 32,600–32,300 cm^{-1} while those of the benzophenone-derived thiosemicarbazones exhibit a band at ca. 31,450–31,350 cm^{-1}. This absorption is attributed to the $\pi \rightarrow \pi^*$ transition of the benzene ring and the $n \rightarrow \pi^*$ transitions of the azomethine and thioamide functions overlapped in the same envelope [22,23]. In the spectra of the zinc(II) complexes two absorptions were observed at ca. 33,780–31,150 cm^{-1} and ca. 30,770–29,940 cm^{-1} for the acetophenone-derived thiosemicarbazones and at ca. 31,250–29,850 cm^{-1} and 27,800–27,300 cm^{-1} for the benzophenone-derived thiosemicarbazones. The first is attributed to the $\pi \rightarrow \pi^*$ transition of the benzene ring and the second to the $n \rightarrow \pi^*$ transitions of C=N and C=S [16]. The two separate absorptions observed in the spectra of the complexes are due to the formation of a highly delocalized system upon deprotonation at N2—H, involving the benzene ring and the thiosemicarbazone chain. Hence the $n \rightarrow \pi^*$ transitions appear at lower energies in the complexes.

3.2.3. NMR spectra

The NMR spectra of the thiosemicarbazones and their zinc(II) complexes were recorded in DMSO-d_6. The ^{1}H resonances were assigned on the basis of chemical shifts and multiplicities. The carbon type (C, CH) was determined by using distortion less enhancement by polarization transfer (DEPT135) experiments.

In the ^{1}H and ^{13}C NMR spectra of HAc3mF (**2**) and HBz3mF (**4**) and their zinc(II) complexes (**6** and **8**) the fluor nucleus couples with neighbor hydrogen and carbon nuclei resulting in splitting of the hydrogen and carbon signals. In the ^{1}H NMR spectra of all complexes the signal of N2—H is absent due to deprotonation and formation of an anionic ligand. The signals of N3—H undergo significant shifts in relation to their position in the free thiosemicarbazones, indicating coordination through the sulfur. The signals of CH_3 from the acetophenone group shift significantly upon complexation suggesting coordination through the imine nitrogen [22]. Upon coordination significant shifts were observed in the ^{13}C NMR signals especially for C2, C=N, C=S and C9, which also confirms coordination of the thiosemicarbazone through the imine nitrogen and the sulfur in the thiolate form [9,24].

3.2.4. X-ray crystallography

In the structure of HAc3*m*F (**2**) the thiosemicarbazone backbone is almost planar with a mean plane deviation of 0.0293 Å. The compound adopts the *EE* conformation in relation to the C7=N1 and C8—N2 bonds [25] (see Fig. 2). In the molecular packing dimmers are generated by pairs of N—H···S hydrogen bonds (d(D···A) = 3.8135 (16) Å; ∠(DHA) = 175.7°) related to each other by an inversion center [26] (Fig. 2).

Fig. 3 shows the molecular structures of [Zn(Ac3*m*Cl)$_2$] (**5**) and [Zn(Bz3*m*F)$_2$]·DMSO (**8a**). The asymmetric unit of **5** contains half of a [Zn(Ac3*m*Cl)$_2$] molecule. In [Zn(Bz3*m*F)$_2$]·DMSO (**8a**) the *meta*-fluorphenyl ring and the DMSO solvent molecules have shown to be twofold disordered; the refined occupancies converged to 72:28 and 54:46, respectively. We may suspect that the structure of **8a** would present higher symmetry in the absence of DMSO and of the disorder in the *meta*-fluorphenyl ring. In fact the distances and angles in the two ligands of complex (**8a**) are not significantly different (see Table 2).

Selected intra-molecular bond distances and angles in the structures of HAc3*m*F (**2**), [Zn(Ac3*m*Cl)$_2$] (**5**) and [Zn(Bz3*m*F)$_2$]·DMSO (**8a**) are given in Table 2.

In complexes (**5**) and (**8a**) two anionic thiosemicarbazones are attached to the zinc(II) center through the N—S chelating system. The geometry around the metal is highly distorted tetrahedral. The small N1—Zn1—S1 (**5**) and N1—Zn1—S11, N11—Zn1—S101 (**8a**) angles (86.5–87.5°) are very different from the expected angle of 109° for a perfect tetrahedron, probably due to the rigidity of the thiosemicarbazone's N—S chelating system [27]. As a consequence the N1—Zn1—S1′- (**5**) and N1—Zn1—S101, N11—Zn1—S1 (**8a**) angles are 137.45(9)° in **5** and 129.02(4)°, 128.81(4)° in **8a**. The sum of the N1—Zn1—S1, N1—Zn1—S1′, N1′—Zn1—S′, N1′—Zn1—S1 angles is 442.7° for complex (**5**) and the sum of the equivalent angles in complex (**8a**) are 446.16° and 445.38°, while the sum of the four angles of a perfect tetrahedron is 437.88°. Hence, as already mentioned, the geometries of **5** and **8a** are highly distorted tetrahedral.

In complexes (**5**) and (**8a**) the coordinated thiosemicarbazone adopts the *EZ* conformation in relation to the C7—N1 and N2—C8 bonds.

Comparison between complexes (**5**) and (**8a**) reveals that the two compounds present comparable bond distances. In general the bond angles of the thiosemicarbazone chain in the two complexes are also not significantly different. However, the angles comprising the metal are not similar.

Considering that the bond distances do not significantly vary in complexes (**5**) and (**8a**) in spite of the fact that **5** contains a chloro substituent while **8a** contains a fluor substituent at the *N*(3)-phenyl group, comparisons of bond distances could in principle be made

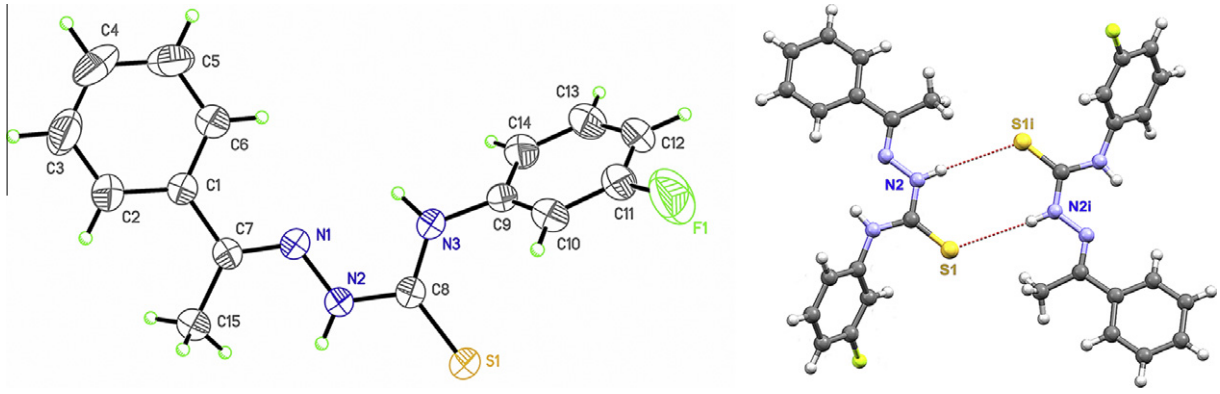

Fig. 2. Molecular structure of HAc3*m*F (**2**) showing the labelling scheme of the non-H atoms and their displacement ellipsoids at the 50% probability level (left) together with the N—H···S hydrogen bonds indicated by dashed lines (right).

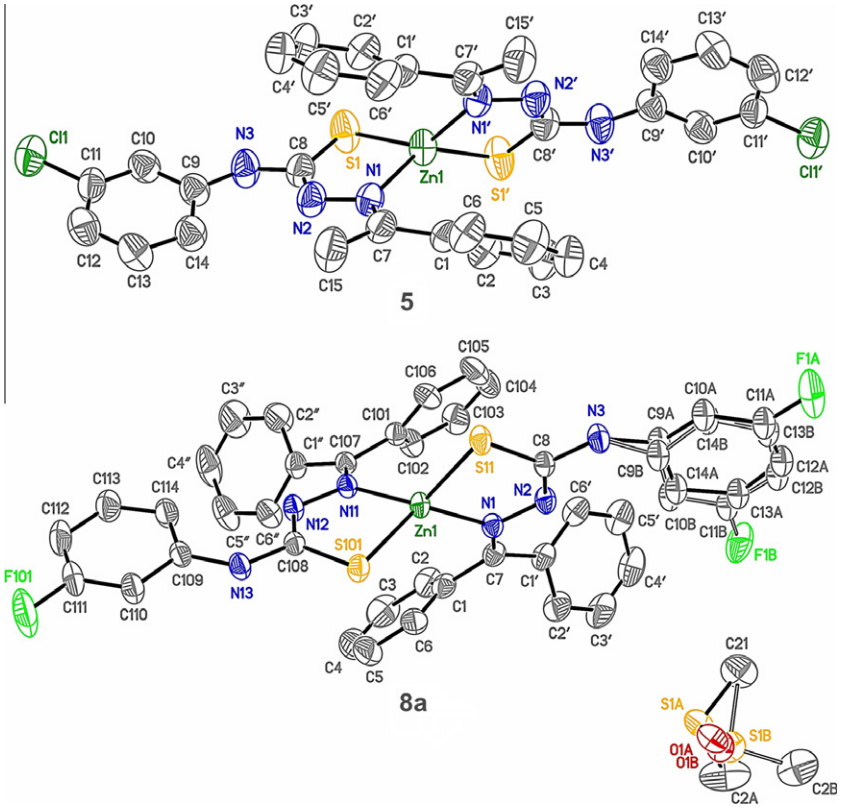

Fig. 3. Molecular structures of $[Zn(Ac3mCl)_2]$ (**5**) and $[Zn(Bz3mF)_2]$·DMSO (**8a**) showing the labelling scheme of the non-H atoms and their displacement ellipsoids at the 50% probability level. In **5**, the "prime" atoms were generated by $[-x, y, -z + 1/2]$.

Table 2
Selected bonds distances (Å), and angles (°) for HAc3*m*F (**2**), $[Zn(Ac3mCl)_2]$ (**5**) and $[Zn(Bz3mF)_2]$·DMSO (**8a**). Standard deviation in parenthesis.

Atoms	(2)	Atoms	(5)	Atoms	(8a)
Distance (Å)					
–	–	Zn1—N1	2.075(3)	Zn1—N1/Zn1—N11	2.0537(14)/2.0566(14)
–	–	Zn1—S1	2.2884(11)	Zn1—S101/Zn1—S11	2.2849(5)/2.2726(5)
S1—C8	1.670(2)	S1—C8	1.738(4)	S11—C8/S101—C108	1.7513(18)/1.7470(17)
N1—C7	1.281(2)	N1—C7	1.309(5)	N1—C7/N11—C107	1.304(2)/1.302(2)
N1—N2	1.374(2)	N1—N2	1.387(4)	N1—N2/N11—N12	1.391(2)/1.3885(19)
N2—C8	1.354(2)	N2—C8	1.283(5)	N2—C8/N12—C108	1.298(2)/1.302(2)
N3—C8	1.341(3)	N3—C8	1.379(5)	N3—C8/N13—C108	1.369(2)/1.365(2)
Angles (°)					
–	–	N1′—Zn1—N1	107.80(16)	N1—Zn1—N11	115.01(6)
–	–	S1′—Zn1—S1	111.82(6)	S101—Zn1—S11	114.561(19)
–	–	N1—Zn1—S1	85.63(8)	N1—Zn1—S11/N11—Zn1—S101	87.57(4)/87.00(4)
–	–	N1—Zn1—S1′	137.45(9)	N1—Zn1—S101/N11—Zn1—S1	129.02(4)/128.81(4)
–	–	C8—S1—Zn1	93.21(14)	C8—S11—Zn1/C108—S101—Zn1	92.30(6)/92.47(6)
C7—N1—N2	118.94(17)	C7—N1—N2	113.9(3)	C7—N1—N2/C107—N11—N12	115.28(14)/114.87(14)
N1—N2—C8	119.17(16)	N1—N2—C8	115.2(3)	N1—N2—C8/N11—N12—C108	115.90(14)/116.00(14)
N2—C8—S1	119.81(15)	N2—C8—S1	129.0(3)	N2—C8—S11/N12—C108—S101	128.44(13)/128.17(13)
S1—C8—N3	125.62(15)	N3—C8—S1	113.1(3)	N3—C8—S11/N13—C108—S101	113.64(13)/113.97(13)
N3—C8—N2	114.52(17)	N3—C8—N2	117.9(4)	N2—C8—N3/N12—C108—N13	117.91(16)/117.86(15)

[a] Symmetry operation: ′ = $-x, y, -z + 1/2$.

between HAc3*m*F (**2**) and the acetophenone thiosemicarbazone complex (**5**). C8—S1, which is a predominantly double bond, varies from 1.670(2) Å in **2** to 1.738(4) Å in **5** as a consequence of deprotonation with formation of a new predominantly single bond [28]. The N2—C8 bond goes from 1.354(2) Å in **2** to 1.283 (5) Å in **5** due to this same effect. Significant modifications were observed as well in the bond angles involving the sulfur atom in **2** and **5**.

We were not able to grow crystals of complexes (**6**) and (**7**) but considering that both **5** and **8a** are highly distorted tetrahedral we may assume that **6** and **7** probably present the same geometry.

4. Conclusions

N(3)-*meta*-chlorophenyl- and *N*(3)-*meta*-fluorphenyl thiosemicarbazones derived from acetophenone and benzophenone coordinate to zinc(II) forming $[Zn(L_2)]$ (L = anionic thiosemicarbazone) complexes, in which the bidentate thiosemicarbazone ligands adopt the *EZ* conformation in relation to the C7—N1 and N2—C8 bonds.

The presence of triethylamine in the reaction mixture induced deprotonation at N(2)—H and the excess of zinc(II) probably

favored formation of tetrahedral [$Zn(L_2)$] (L = anionic thiosemicarbazone) instead of octahedral [$Zn(L)_3$] complexes. In addition, since the d^{10} configuration of zinc(II) affords no crystal field stabilization, the presence of rather bulky thiosemicarbazone ligands also probably contributed to the formation of tetrahedral species. Moreover, the rigidity of the thiosemicarbazone's N—S chelating system is responsible for the highly distorted tetrahedral geometry of the complexes.

Appendix A. Supplementary material

CCDC 844586, 844587 and 844588 contain the supplementary crystallographic data for thiosemicarbazone (**2**) and complexes (**5**) and (**8a**). These data can be obtained free of charge via http://www.ccdc.cam.ac.uk/conts/retrieving.html, or from the Cambridge Crystallographic Data Centre, 12 Union Road, Cambridge CB2 1EZ, UK; fax: (+44) 1223 336033; or e-mail: deposit@ccdc.cam.ac.uk. Supplementary data associated with this article can be found, in the online version, at doi:10.1016/j.molstruc.2011.11.035.

References

[1] H. Beraldo, D. Gambino, Mini Rev. Med. Chem. 4 (2004) 159.
[2] R.A. Finch, M.C. Liu, S.P. Grill, W.C. Rose, R. Loomis, K.M. Vasquez, Y.C. Cheng, A.C. Sartorelli, Biochem. Pharmacol. 59 (2000) 983.
[3] D. Kovala-Demertzi, P.N. Yadav, J. Wiecek, S. Skoulika, T. Varadinova, M.A. Demertzis, J. Inorg. Biochem. 104 (2010) 467.
[4] N.C. Kasuga, K. Sekino, M. Ishikawa, A. Honda, M. Yokoyama, S. Nakano, N. Shimada, C. Koumo, K. Nomiya, J. Inorg. Biochem. 96 (2003) 298.
[5] N. Farrell, Coord. Chem. Rev. 232 (2002) 1.
[6] W. Maret, BioMetals 22 (2009) 149.
[7] G.K. Walkup, S.C. Burdette, S.J. Lippard, R.Y. Tsien, J. Am. Chem. Soc. 122 (2000) 5644.
[8] D. Kovala-Demertzi, P.N. Yadav, J. Wiecek, S. Skoulika, T. Varadinova, M.A. Demertzis, J. Inorg. Biochem. 100 (2006) 1558.
[9] J.G. Da Silva, S.M.S.V. Wardell, J.L. Wardell, H. Beraldo, J. Coord. Chem. 62 (2009) 1400.
[10] CRYSALISPRO, Oxford Diffraction Ltd., Version 1.171.34.34 (release 05-01-2010 CrysAlis171.NET).
[11] G.M. Sheldrick, Acta Crystallogr. A64 (2008) 112.
[12] V.T. Siatra-Papastaikoudi, A. Tsotinis, C.P. Raptopoulou, C. Sambani, H. Thomou, Eur. J. Med. Chem. 30 (1995) 107.
[13] L.J. Farrugia, J. Appl. Crystallogr. 30 (1997) 565.
[14] A.L. Spek, Acta Crystallogr. D65 (2009) 148.
[15] D.X. West, A. Castineiras, E. Bermejo, J. Mol. Struct. 520 (2000) 103.
[16] E.B. Seena, K. Prathapachandra, Spectrochim. Acta Part A 69 (2008) 726.
[17] D.X. West, I.S. Billeh, J.P. Jasinski, J.M. Jasinski, R.J. Butcher, Transition Met. Chem. 23 (1998) 209.
[18] I.C. Mendes, J.P. Moreira, A.S. Mangrich, S.P. Balena, B.L. Rodrigues, H. Beraldo, Polyhedron 26 (2007) 3263.
[19] K. Alomar, A. Landreau, M. Kempf, M.A. Khan, M. Allain, G. Bouet, J. Inorg. Biochem. 104 (2010) 397.
[20] A.A.R. Despaigne, J.G. Da Silva, A.C.M. Do Carmo, O.E. Piro, E.E. Castellano, H. Beraldo, J. Mol. Struct. 920 (2009) 97.
[21] G.L. Parrilha, R.P. Vieira, A.P. Rebolledo, I.C. Mendes, L.M. Lima, E.J. Barreiro, O.E. Piro, E.E. Castellano, H. Beraldo, Polyhedron 30 (2011) 1891.
[22] H. Beraldo, W.F. Nacif, L.R. Teixeira, J.S. Rebouças, Transition Met. Chem. 27 (2002) 85.
[23] H. Beraldo, R. Lima, L.R. Teixeira, A.A. Moura, D.X. West, J. Mol. Struct. 559 (2001) 99.
[24] T.P. Stanojkovic, D. Kovala-Demertzi, A. Primikyri, I. Garcia-Santos, A. Castineiras, Z. Juranic, M.A. Demertzis, J. Inorg. Biochem. 104 (2010) 467.
[25] J.S. Casas, M.S. García-Tasende, J. Sordo, Coord. Chem. Rev. 209 (2000) 197.
[26] J.A. Lessa, I.C. Mendes, P.R.O. da Silva, M.A. Soares, R.G. Santos, N.L. Speziali, N.C. Romeiro, E.J. Barreiro, H. Beraldo, Eur. J. Med. Chem. 45 (2010) 5671.
[27] L. Latheef, E. Manoj, M.R.P. Kurup, Polyhedron 26 (2007) 4107.
[28] K.S.O. Ferraz, L. Ferandes, D. Carrilho, M.C.X. Pinto, M.F. Leite, E.M. Souza-Fagundes, N.L. Speziali, I.C. Mendes, H. Beraldo, Bioorg. Med. Chem. 17 (2009) 7138.